

# How to define the boundaries of a convective zone and how extended is overshooting?

L. Deng<sup>1</sup> & D.R. Xiong<sup>2</sup>

<sup>1</sup>National Astronomical Observatories, Chinese Academy of Sciences, Beijing 100012; [licai@bao.ac.cn](mailto:licai@bao.ac.cn)

<sup>2</sup>Purple Mountain Observatory, Chinese Academy of Sciences, Nanjing 210008; [Xiongdr@pmo.ac.cn](mailto:Xiongdr@pmo.ac.cn)

8 December 2021

## ABSTRACT

Under nonlocal convection theory, convection extends without limit therefore no apparent boundary can be defined clearly as in the local theory. From the requirement of a similar structure for both local and non-local models having the same depth of convection zone, and taking into account the driving mechanism of turbulent convection, we argue that a proper definition of the boundary of a convective zone should be the place where the convective energy flux (i.e. the correlation of turbulent velocity and temperature) changes its sign. Therefore, it is convectively unstable region when the flux is positive, and it is convective overshooting zone when the flux becomes negative. The physical picture of the overshooting zone drawn by the usual non-local mixing-length theory is not correct. In fact, convection is already sub-adiabatic ( $\nabla < \nabla_{ad}$ ) far before reaching the unstable boundary; while in the overshooting zone below the convective zone, convection is sub-adiabatic and super-radiative ( $\nabla_{rad} < \nabla < \nabla_{ad}$ ). The transition between the adiabatic temperature gradient and the radiative one is continuous and smooth instead of a sudden switch. In the unstable zone the temperature gradient is approaching radiative rather than going to adiabatic. We would like to claim again that, the overshooting distance is different for different physical quantities. In a overshooting zone at deep stellar interiors, the e-folding lengths of turbulent velocity and temperature are about  $0.3H_P$ , whereas that of the velocity-temperature correlation is much shorter, being about  $0.09H_P$ . The overshooting distance in the context of stellar evolution, measured by the extent of mixing of stellar matter, should be more extended. It is estimated as large as 0.25-1.7  $H_p$  depending on the evolutionary timescale. The larger the overshooting distance, the longer the timescales. This is due to the participation of extended overshooting tail in the mixing process.

**Key words:** convection—stars:evolution

## 1 INTRODUCTION

As the classical treatment of convection, the local theory has been used in modelling stellar structure and evolution. In the calculation of massive star evolution, Schwarzschild & Härm (1958) discovered that the hydrogen rich radiative envelope just outside the helium rich convective core cannot be convectively stable, and that led to the paradox of so called semi-convection. To solve that problem, the idea of semi-convection was initiated, i.e. the region outside the convective core is in a state of semi-convection. Stellar matter in this region is nearly in neutral stability ( $\nabla \leq \nabla_{ad}$ ), therefore convective energy transport due to this mild convection can be neglected, while the mixing of chemical compositions should be important, which makes a gradient of molecular weight in this region (otherwise called semi-convection zone). There had been a great debate in the community for a long period since then on whether the Schwarzschild or

Ledoux criteria should be applied for the neutral stability of convection, and whether the semi-convective zone should be very wide or rather narrow. Stothers (1970) commented on various establishments of semi-convection. Evolutionary scenarios for massive stars with or without semi-convection were also discussed (eg. Chiosi & Summa 1970). It has been realized later that the problem of semi-convection is in fact due to the non-locality of stellar convection. Therefore various theories of non-local theory of stellar convection have been worked out (Spiegel 1963, Ulrich 1970, Xiong 1977, 1981a, 1989, Kufuss 1986, Grossman et al 1993, Canuto 1993, Canuto & Dubovikov 1998). Such non-local theories of stellar convection have then been applied in the studies of structures of the solar and stellar convective envelopes (Travis & Matsushima 1973, Unno et al. 1985, Xiong & Cheng 1992), stellar oscillations (Xiong 1981b, Xiong, Deng & Cheng 1998, Xiong, Cheng & Deng 1998, Xiong & Deng

2001, 2007) and stellar evolution (Xiong 1986). Generally speaking, non-local theory of convection makes the results better match observations than the local ones. However, the non-local theory of convection is rather complicated, which is much less straightforward to be understood, much more difficult to be applied and much more computing power demanding than the phenomenological local (Böhm-Vitense 1958) and non-local mixing length theories (Maeder 1975, Bressan et al. 1981). For these reasons, it becomes a general practice to use the phenomenological local or non-local mixing length treatment for stellar convection in nowadays stellar evolution models. The non-local mixing of chemical compositions during the evolution of stars is dealt with by attaching a parametric overshooting zone outside the convectively unstable region. The parametric distance of convective overshooting has a great impact on the properties of stellar evolution. The goal of present work is to discuss the calibration of the overshooting distance. The physical definition of the boundary of the convective zone is discussed in the next section. In section 3, calibrations of the overshooting distance by numerical simulations of non-local convection and depletion of solar Lithium abundance are presented. A summary and discussions are given in the last section.

## 2 HOW TO DEFINE THE BOUNDARIES OF A CONVECTIVE ZONE?

Normally in a local theory of convection, the boundary of convective zone is given by the so called Schwarzschild's criterion,

$$\nabla = \nabla_{ad}, \quad (1)$$

which is derived by analysis of the local convective stability. However, if viewed from hydrodynamics strictly, all hydrodynamic phenomena including convective motions in stars are non-local, therefore there should be no well defined boundary for convective motion in an extended medium. In a certain sense, forcing a definition of boundary for a convective zone is always an artifact. Defining a boundary for stellar convection is needed in practice of stellar evolution calculations, but this cannot be done arbitrarily, instead some objective standards should be respected. These standards should at least include the following:

(i) As a matter of fact, most of calculations for stellar structure and evolution still use local theory of convection. Therefore, the definition of boundary given by a non-local convection theory should be kept as close as possible to that by a local theory. In other words, the local and non-local convection models with the same depth of convective zone should be made to have structures as similar as possible.

(ii) the definition of the boundary should be physically pounced in any case, i.e. the unstable convective zone should be the driving (excitation) region of convective motion, and the adjacent overshooting zone should be the dissipation region of convective motion.

Stellar convection happens due to some internal instability of the thermal structure in gravitationally stratified fluid, therefore the study of the resulted convective motions should be based on the dynamical equations of fluid. A complete dynamic equations of time-dependent non-local con-

vection theory can be found in our previous work (Xiong 1981, 1989). For the sake of clarity, and to make it easier to read this paper, the derivation of the dynamic equations of turbulent convection in steady fluid is presented here. The conservations of momentum and energy of fluid dynamics can be expressed as,

$$\begin{aligned} \frac{\partial(\rho u^i)}{\partial t} + \nabla_k(\rho u^i u^k + g^{ik}P) \\ + \rho g^{ik} \nabla_k \phi = \nabla_k \sigma^{ik}(u), \end{aligned} \quad (2)$$

$$\begin{aligned} \frac{\partial(\rho H)}{\partial t} + \nabla_k(\rho u^k H) - \frac{\partial P}{\partial t} \\ - u^k \nabla_k P + \nabla_k F_r^k = \rho \epsilon_N + \sigma^{ik}(u) \nabla_k u_i, \end{aligned} \quad (3)$$

where  $\rho$ ,  $T$  and  $P$  are the regular labels for density, temperature and pressure (including radiative pressure) of gas;  $H$  and  $\epsilon_N$  are enthalpy and nuclear energy generation rate per unit mass;  $u^i$  is the  $i$ th component of fluid motion vector;  $\sigma^{ik}(u)$  the viscous stress tensor;  $F_r^i$  is  $i$ th component of the radiative flux vector. The implicit summation rule of tensor calculations is used, i.e. a pair of sub- and super-script index means summation from 1 to 3. When convection happens, any physical quantity can be written as the sum of averaged and turbulent fluctuated components as,

$$X = \bar{X} + X'. \quad (4)$$

Putting the expressions of all quantities in the form of eq. (4) into eqs. (2)–(3), and averaging the whole equations, the dynamic equations for the mean flow can be derived as,

$$\begin{aligned} \frac{\partial(\bar{\rho} \bar{u}^i)}{\partial t} + \nabla_k(\bar{\rho} \bar{u}^i \bar{u}^k + \overline{\rho u'^i u'^k} + g^{ik} \bar{P}) \\ = \nabla_k \sigma^{ik}(\bar{u}), \end{aligned} \quad (5)$$

$$\begin{aligned} \frac{\partial(\bar{\rho} \bar{H})}{\partial t} + \nabla_k(\bar{\rho} \bar{u}^k \bar{H} + \overline{\rho u'^k H'}) \\ - \frac{\partial \bar{P}}{\partial t} - \bar{u}^k \nabla_k \bar{P} - \overline{u'^k \nabla_k P} + \nabla_k \bar{F}_r^k \\ = \bar{\rho} \bar{\epsilon}_N + \overline{\sigma^{ik}(u) \nabla_k u_i}. \end{aligned} \quad (6)$$

Subtracting the corresponding equations of the mean motion eqs. (5)–(6) from eqs. (2)–(3), and considering the static state of the flow, i.e.

$$\bar{u} = \frac{\partial \bar{P}}{\partial t} = \frac{\partial \bar{\rho}}{\partial t} = \frac{\partial \bar{H}}{\partial t} = 0, \quad (7)$$

the dynamic equations for the fluctuation quantities can be derived as,

$$\begin{aligned} \frac{\partial w'^k}{\partial t} + \frac{1}{\bar{\rho}}(g^{ik} P' + \rho u'^i u'^k - \overline{\rho u'^i u'^k}) \\ + g^{ik} \left[ \frac{\rho'}{\bar{\rho}} \nabla_k \bar{\Phi} + \nabla_k \Phi' \right] = \frac{1}{\bar{\rho}} \nabla_k \sigma^{ik}(u'), \end{aligned} \quad (8)$$

$$\begin{aligned} \frac{\partial}{\partial t}(\rho H' + \rho' \bar{H}) + \nabla_k(\rho u'^k \bar{H}' - \overline{\rho u'^k H}) \\ - \frac{\partial P'}{\partial t} - u'^k \nabla_k P + \overline{u'^k \nabla P} \end{aligned}$$

$$\begin{aligned}
 &= \rho \epsilon'_N + \rho' \epsilon_{\bar{N}} - \nabla_k F_r'^{ik} \\
 &+ \sigma^{ik} (u') \nabla_k u'_i - \overline{\sigma^{ik} \nabla_k u_i}.
 \end{aligned} \tag{9}$$

By using a certain thermodynamic relations, and following some deductions and simplifications, eq. (9) can be written as,

$$\begin{aligned}
 &\frac{\partial}{\partial t} \left( \frac{T'}{\bar{T}} \right) + w'^k (\nabla_k \ln \bar{T} - \nabla_{ad} \nabla_k \ln \bar{P}) \\
 &+ \frac{1}{\bar{\rho} \bar{C}_P \bar{T}} \left\{ u'^k \nabla_k P + \nabla_k \left[ \bar{\rho} \bar{C}_P \bar{T} \left( w'^k \frac{T'}{\bar{T}} - \overline{w'^k \frac{T'}{\bar{T}}} \right) \right] \right\} \\
 &= \frac{1}{\bar{\rho} \bar{C}_P \bar{T}} \left[ \nabla_k F_r'^{ik} + \sigma^{ik} (u) \nabla_k u_i \right],
 \end{aligned} \tag{10}$$

where  $w'$  is the density weighted fluctuation of turbulent velocity,

$$w'^k = \frac{\rho u'^k}{\bar{\rho}}, \tag{11}$$

Starting from eq. (8) and eq. (10), we can have the following dynamic equations for the auto- and cross-correlations of turbulent velocity and temperature fluctuations:

$$\begin{aligned}
 \frac{3}{2} \bar{\rho} \frac{\partial x^2}{\partial t} &= B \frac{GM_r \bar{\rho}}{r^2} V \\
 &+ \bar{\rho} \frac{\partial}{\partial M_r} \left( 4\pi r^2 \overline{\bar{\rho} u'_r w'_i w'^i / 2} \right) - 1.56 \frac{GM_r \bar{\rho}^2 x^3}{c_1 r^2 \bar{P}},
 \end{aligned} \tag{12}$$

$$\begin{aligned}
 \frac{\partial Z}{\partial t} &= 2 \frac{GM_r \bar{\rho}}{r^2 \bar{P}} (\nabla - \nabla_{ad}) V \\
 &+ \frac{1}{\bar{\rho} \bar{C}_P^2} \frac{\partial}{\partial M_r} \left[ 4\pi r^2 \bar{\rho}^2 \bar{C}_P^2 u'_r \overline{\left( \frac{T'}{\bar{T}} \right)^2} \right] \\
 &- 1.56 \frac{GM_r \bar{\rho}}{c_1 r^2 \bar{P}} (x + x_c) Z,
 \end{aligned} \tag{13}$$

$$\begin{aligned}
 \frac{\partial V}{\partial t} &= \frac{GM_r \bar{\rho}}{r^2 \bar{P}} (\nabla - \nabla_{ad}) x^2 + B \frac{GM_r}{r^2} Z \\
 &+ \frac{1}{\bar{C}_P} \frac{\partial}{\partial M_r} \left( 4\pi r^2 \bar{\rho} \bar{C}_P u'_r w'_r \overline{\frac{T'}{\bar{T}}} \right) \\
 &- 0.78 \frac{GM_r \bar{\rho}}{c_1 r^2 \bar{P}} (3x + x_c) V,
 \end{aligned} \tag{14}$$

where  $x^2$ ,  $Z$  and  $V$  are respectively the auto and cross correlations of turbulent velocity  $w'$  and the relative temperature fluctuation  $T'/\bar{T}$ , defined as the following,

$$x^2 = \overline{w'^i w'_i} / 3, \tag{15}$$

$$Z = \overline{\left( T' / \bar{T} \right)^2}, \tag{16}$$

$$V = \overline{w'_r T' / \bar{T}}, \tag{17}$$

while  $\nabla_{ad}$  is the adiabatic temperature gradient,  $\nabla = \partial \ln \bar{T} / \partial \ln \bar{P}$  is the temperature gradient,  $x_c$  is a variable related with the effect of thermal conductivity:

$$x_c = \frac{3ac GM_r \bar{T}^3}{c_1 \bar{\rho} \bar{C}_P \bar{P} r^3}. \tag{18}$$

$P_e = x/x_c$  is the effective Peclet number of turbulent convection.  $\bar{B} = -(\partial \ln \rho / \partial \ln T)_P$  the expansion coefficient of gas. The detailed derivation of the dynamic equations of correlations can be found in our previous work (Xiong 1978, 1981, 1989). Eqs. (12), (13) and (14) are the dynamic equations of turbulent convection in steady fluid, which have very clear physical meanings. Eq. (12), for instance, is for the conservation of turbulent kinetic energy. The left hand side is the rate of variations of turbulent energy per unit volume, which is equal to the sum of the 3 terms on the right hand side: the first term is the work done by buoyant force:

$$W_{buo} = \frac{GM_r \bar{\rho}}{r^2} BV. \tag{19}$$

while the expression in the bracket of the second term represents the effect of non-locality, which is the flux of turbulent kinetic energy  $L_t$ ,

$$L_t = 4\pi r^2 \overline{\bar{\rho} u'_r w'_r w'^i} / 2. \tag{20}$$

Therefore the second term on the right hand side of eq. (12) is the net gaining rate of turbulent kinetic energy per unit volume  $-\bar{\rho} \partial L_r / \partial M_r$ . The third term on the right hand side of eq. (12) is for viscous dissipations, i.e. the dissipation rate  $\bar{\rho} \bar{\epsilon}_1$  by converting turbulent kinetic energy into thermal energy due to viscosity.  $c_1$  is a convection parameter related to the viscous dissipation of turbulent convection.  $l_e = c_1 H_P r / R_0$  is the linear size of the energy-containing eddies (Xiong 1978, 1981a, 1989). Both Eqs. (13) and (14) have similar physical means: the left hand sides are the variation rates of correlations  $Z$  (or  $V$ ) respectively. The first (and the second for eq. [14]) term on the right hand side of eq. (13) [ or eq. (14)] is the rate of increase of  $Z$  (or  $V$ ) due to super-adiabatic temperature gradient (and buoyant force for eq. [14]); the second (the third for eq. [14]) term represents the net increase rate of  $Z$  (or  $V$ ) due to non-local convective energy flux; while the last term describes the turbulent dissipation due to viscosity and thermal conductivity. For static convection, the time derivatives terms on the left hand side of eqs. (12)–(14) all vanish:

$$\frac{\partial x^2}{\partial t} = \frac{\partial Z}{\partial t} = \frac{\partial V}{\partial t} = 0. \tag{21}$$

Hence, eq. (12) can be rewritten as,

$$W_{buo} - \bar{\rho} \frac{\partial L_r}{\partial M_r} - \bar{\rho} \bar{\epsilon}_1 = 0. \tag{22}$$

It is clear from eq. (22) that, for static convection, the net gaining rate of turbulent kinetic energy ( $-\bar{\rho} \partial L_r / \partial M_r$ ) and buoyant force work ( $W_{buo}$ ) will be balanced by turbulent dissipation  $\bar{\rho} \bar{\epsilon}_1$  (the sum of all the three terms vanishes). There is no need to go through the similar physical meanings of eqs. (13) and (14). When neglecting all the third order correlations representing the transportation effect of non-local turbulent convection, eqs. (12)–(14) can be converted to,

$$BV - 1.56 \frac{\bar{\rho}}{c_1 \bar{P}} x^3 = 0, \tag{23}$$

$$(\nabla - \nabla_{ad}) V - \frac{0.78}{c_1} (x + x_c) Z = 0, \tag{24}$$

$$x^2 (\nabla - \nabla_{ad}) + B \frac{\bar{P}}{\bar{\rho}} Z - \frac{0.78}{c_1} (3x + x_c) V = 0, \tag{25}$$

It is rather easy to solve eqs. (23)–(25) for  $x^2$ ,  $Z$  and  $V$ ,

$$x^2 = \frac{1}{2} \left( \frac{c_1}{0.78} \right)^2 \frac{B\bar{P}}{\bar{\rho}} \left( 1 + \frac{x}{x_c} \right)^{-1} (\nabla - \nabla_{ad}), \quad (26)$$

$$Z = \left( \frac{c_1}{0.78} \right)^2 \left( 1 + \frac{x}{x_c} \right)^{-2} (\nabla - \nabla_{ad})^2, \quad (27)$$

$$V = \left( \frac{c_1}{0.78} \right)^2 \left( \frac{B\bar{P}}{2\bar{\rho}} \right)^{1/2} \left( 1 + \frac{x}{x_c} \right)^{-3/2} (\nabla - \nabla_{ad})^{3/2}. \quad (28)$$

Comparing eqs. (26)–(28) and the equations of the local mixing length theory (Bhom-Vitense 1958), and substituting  $c_1$  and the effective Peclet number  $x/x_c$  in our equations by the mixing length parameter  $\alpha$  and  $\gamma$  respectively, it is clear that the two expressions are the same. The stability condition for convection is the Schwarzschild criterion (eq. [1]) in a chemically homogeneous medium. When there is a molecular weight gradient, the neutral stability condition should be Ledoux criterion (Xiong 1981a):

$$\nabla = \nabla_{ad} + \nabla_{\mu}, \quad (29)$$

Hence, viewed from hydrodynamics, the local mixing length theory is only a special simplified case of our statistical theory of correlations for turbulent convection. The third order correlation terms in eqs. (12)–(14) represent non-local effect of turbulent convection, neglecting which makes the equations becoming the local expressions eqs. (23)–(25) or their explicit form eqs. (26)–(28). In this case, a convective zone will have a clearly defined boundary given by Schwarzschild (or Ledoux) criterion:  $\nabla > \nabla_{ad}$  is convectively unstable, while  $\nabla < \nabla_{ad}$  stable (radiative). As we shall show later, within the convectively unstable ( $V > 0$ ) zone far away from the boundary, the third order correlation terms in eqs. (12)–(14) can be safely neglected compared with other terms. This means that the local expression of convection is a fairly good first approximation at the deep interior of an unstable zone. This is exactly the reason why the mixing length theory is still widely applied in the calculations of stellar structures. However, when studying the entirety of a convective zone, especially near the boundary of convective zone and in the overshooting region, the third correlation terms cannot be neglected. Instead, they are the true reasons for the existence of convective overshooting. In the non-local convection theory, it is clear from eqs. (12)–(14) that the turbulent velocity and temperature fluctuations are different from zero everywhere,

$$x > 0; \quad Z > 0. \quad (30)$$

These conditions make it difficult and uncertain to define a boundary of a convective zone. Schwarzschild criterion is overwhelmingly used in the community to fix the boundary. They think that the temperature gradient is very near and slightly higher than the adiabatic temperature gradient in the unstable region; and is also near but slightly lower than the adiabatic one within the overshooting zone. We are going to show that such a picture for convective overshooting is not correct following the dynamical theory of turbulent convection. The cause of such a mistake is that there is a implicit hypothesis that has been applied in the phenomenological mixing length theory: turbulent velocity is fully correlated (either positively or inversely) with temperature (see eg. Xiong & Cheng 1992, Petrovay & Marik

1995). In fact, when convection is very effective (the effective Peclet number  $x/x_c \gg 1$ ), the correlation between turbulent velocity and temperature fluctuations near the boundary and in the overshooting zone decreases very quickly and vanishes eventually (Xiong & Cheng 1992).

Eqs. (12)–(14) are derived under rather general conditions among which are two important assumptions as the following:

(i) convection is subsonic, the relative fluctuations of temperature and density are both far less than unity:

$$|\rho'/\bar{\rho}| \ll 1; \quad |T'/\bar{T}| \ll 1, \quad (31)$$

(ii) inelastic approximation which actually filters out all acoustic waves not important for energy transfer in subsonic convection.

It is well known that the dynamic equations of turbulent correlations have no closure due to the nonlinearity of hydrodynamics. That means: the third order correlations must be present in the dynamic equations of the second order correlations; while the fourth order ones bound to turn up in the equations of the third order ones, and so forth. Some hypothesis must be used in order to make a closure for the dynamic equations of the correlations. Obviously, the closure cannot be unique. Quite a few methods have been adopted so far (Xiong 1981a, 1989a, Canuto 1993, Grossman et al. 1993, Canuto & Dubvikov 1998). In our opinion, a good closure should meet the following conditions:

(i) the solutions of the resulted equations must be physically sensible. For instance, the standard quasi-normal approximation seems to be better in terms of mathematics, however it gives solutions like  $x^2 < 0$  or  $Z < 0$  which are physically non-sense (Grossman 1996). Such a seemingly reasonable assumption, if not modified somehow, cannot be used for the closure of the dynamical equations of the third order correlations;

(ii) the solutions presented should not be in contradiction with observations. For instance, it should reproduce the main observational properties of solar granular velocity field, it should be able to explain the pulsation instabilities of low temperature stars having extended convective envelope, and it should be able to model the observed Lithium abundance patterns in the atmospheres of the Sun and solar type stars, and so on;

(iii) the solutions provided should be comparable to that of direct hydrodynamical simulations.

Our non-local theory of convection (Xiong 1981a, 1989a) have been tested against the above standards, quite satisfactory results have been reached, therefore we have good reason to believe that it has nicely expressed the dynamic behaviors of stellar turbulent convection.

The solid line in fig. 1 shows the fractional convective flux  $L_c/L$  versus depth  $\log P$  for a model of the solar convective zone calculated with our non-local convection theory, and the dashed line is that of a local convection model having the same depth of convective zone. It follows from the figure that there is almost no difference between the local and non-local model, except some sizable deviations near the boundary of the convective zone; Fig. 2 depicts the relative squared sound speed and density difference between the local and non-local solar convection zone models with

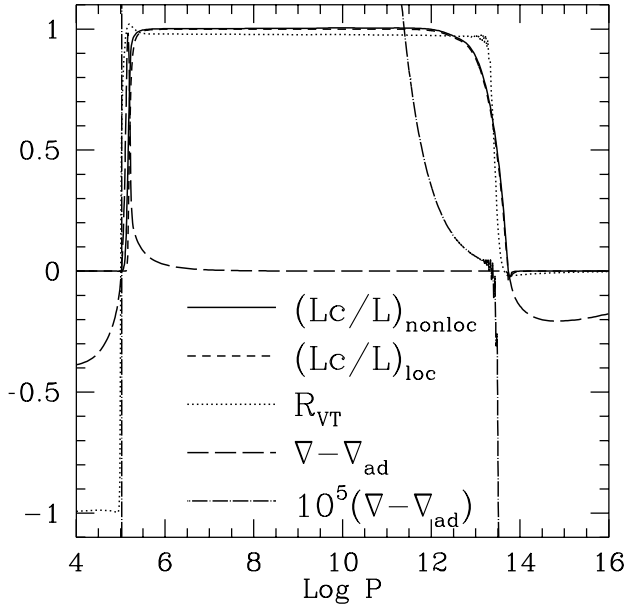


**Figure 1.** The super-adiabatic temperature gradient  $\nabla - \nabla_{\text{ad}}$ , turbulent velocity-temperature correlation  $R_{VT}$ , and the fractional convective flux  $L_c/L$  versus the depth ( $\log P$ ) for a non-local convection model of the Sun. The dashed line is the fractional convective flux  $L_c/L$  for a local model with the same depth of convective zone.

the same depth of convective zone versus depth. The relative difference between the two models is mostly below 1% excluding the solar surface region. In this case, the boundary of the (non-local) convective zone is set at where the turbulent velocity-temperature correlation vanishes,

$$V = 0; \quad (32)$$

Passing through the boundary,  $V$  changes its sign: within the convective zone:

$$V > 0, \quad (33)$$

and in the overshooting zone:

$$V < 0. \quad (34)$$

It is clear from Figs. 1 and 2 that if the boundary is defined as such, the structures of the local and non-local convection models with the same depth of convective zone should be similar. It can be understood by the fact that, within the stellar interior, the turbulent kinetic energy flux ( $L_t$ ) is generally much less than that of thermal convection ( $L_c$ ), and the turbulent pressure ( $P_t = \rho x^2$ ) is much less than that of gas ( $P_g$ ). It can be easily shown that  $P_t/P_g \sim x^2/C_s^2 = Ma^2$ , where  $C_s$  is the local sound speed,  $Ma$  is the Mach number of turbulence;  $L_t/L_c$  is of the same order of magnitude as that of  $P_t/P_g$ . Except at the top of convective zone, we have  $Ma \ll 1$ . It follows from fig. 3 that, for the Sun,  $L_t/L < 1\%$ , therefore the thermal convection  $L_c$  dominates the pressure-temperature (P-T) structure. It is then clear that, when defining the boundary of convective zone by  $V$  changing its sign, the structures of the local and non-local models having the same depth of convective zone will be similar.

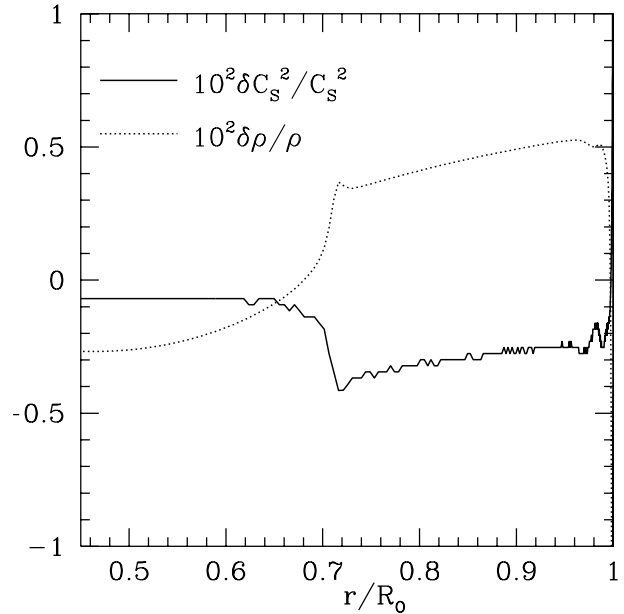


**Figure 2.** The relative differences in the squared sound speed and density between the non-local and the local convection models with the same depth of the convective zone versus the fractional radius.

Fig. 1 clearly demonstrates that convective motions near both upper and lower boundaries of the convective zone are very different. This is due to the fact that, in the atmosphere, the density is very low and  $Pe = x/x_c < 1$ , therefore convective energy transfer is inefficient. As a result, there exists a thin super-adiabatic layer atop of the convective zone. Passing through the upper boundary, the turbulent velocity-temperature correlation  $R_{VT} = V/xZ^{1/2}$  drops quickly from  $\sim 1$  to  $\sim -1$ . This theoretical prediction agrees the observations of solar granular velocity field (Leighton et al. 1962; Salucci et al. 1994) and the results of hydrodynamic simulations (Kupka 2003). Contrary to the situations in the solar atmosphere, convection is highly efficient in terms of energy transfer ( $Pe \gg 1$ ) in the deep interiors of the Sun. Towards the lower boundary of the convective zone, the turbulent velocity-temperature correlation  $R_{VT}$  decreases abruptly and approaches zero ( $|R_{VT}| \ll 1$ ). What makes it so different at the two boundaries is the distinct the effective Peclet number.

Fig. 3a shows the work done by buoyant force  $\rho W_{buo}$ , the net gain ( $> 0$ ) or loss ( $< 0$ ) of turbulent kinetic energy due to non-localism of turbulence  $-\rho \partial L_r / \partial M_r$  and turbulent viscous dissipation rate  $\rho \epsilon$  as functions of depth in the solar convective zone. As shown in fig. 3a, contribution due to non-local convection is much less than the other two quantities in the convective zone, except in the narrow regions near the boundary of convective zone and in the overshooting zones. The energy balance in the bulk of convective zone is due to the interplay of the work done by buoyant force  $W_{buo}$  and the viscous dissipation  $\rho \epsilon$ . Turbulence retrieves energy from buoyant force, while at the same time it dissipates energy due to viscosity. The former factor, as the source, originates primarily from large eddies; while the later one is happening in the viscous dissipation range of the high-

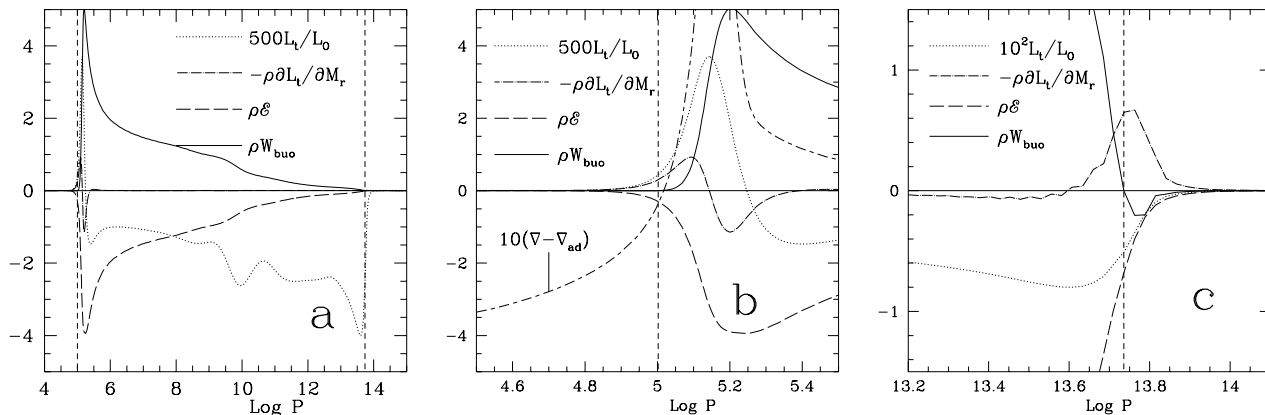


**Figure 3.** a). the work done by buoyant force, viscous dissipation of turbulence  $\rho\epsilon$ , fractional turbulent kinetic energy flux  $L_t/L$  and the net gaining rate of kinetic energy due to turbulent diffusion  $-\rho\partial L_t/\partial M_r$  versus depth ( $\log P$ ) for a non-local solar model. b). and c). are the expanded plots near the upper and lower boundaries of convective zone indicated by the vertical dashed lines.

est end of the turbulent spectrum: turbulence gains energy from buoyant force, which is then cascaded from lowest to higher and higher wave numbers of turbulent spectrum, and is eventually converted into thermal energy due to molecular viscosity. It follows from fig. 3a that the work done by buoyant force  $\rho W_{buo}$  and the viscous dissipation amount nearly the same but have opposite sign within the convectively unstable region.

Figs. 3b and 3c is the enlargements of fig. 3a around the two boundaries. Learnt from the two plots, attention should be paid to the following two points:

(i) In the overshooting zone, both  $\epsilon$  and  $W_{buo}$  are negative, while  $dL_r/dM_r > 0$ . Therefore it is the non-local convective diffusion that drives overshooting, without which there would be no overshooting;

(ii) Before reaching the boundary from the unstable side, the super-adiabatic temperature gradient has already become negative, which is more prominent near the lower boundary of the convective zone (as in fig. 4). The boundary of convective zone ( $V = 0$ ) is located at  $\log P = 13.74$  (the vertical dashed line), but at  $\log P \approx 13.34$  still in the unstable zone, convection is already sub-adiabatic ( $\nabla - \nabla_{ad} < 0$ , see also fig. 1). This is distinctly different from the phenomenological non-local mixing length theories. Although it is resulted from our special non-local mixing length theory, such properties of convection ought to be general. This can be proved by eq. (14) of the general dynamic equations of turbulent convection: The first two terms on the right hand side of eq. (14) are both positive ( $x, Z > 0$ ). As discussed already, the third order correlations representing the non-locality of convection can be neglected compared with the second order terms in the deep interior of convective zone. Therefore, when  $V$  becomes zero (the fourth term on the right hand side), the super-adiabatic temperature gradient must be negative ( $\nabla - \nabla_{ads} < 0$ ) to make the equation mathematically right. This proves that  $\nabla - \nabla_{ad}$  must turn negative before  $V$  does approaching the boundary. This nature of non-local convection does not depend on the kind of non-local convection theory used, which is universally shared by all theories of non-local convection following hydrodynamics.

### 3 HOW EXTENDED IS CONVECTIVE OVERSHOOTING

Due to the complexity of non-local convection theory, almost all the modellings of stellar structure and evolution are still using the local convection theory. Convective overshooting is defined as the penetration of convective motion through the classical boundary of convectively unstable zone into the adjacent stable region. The extent of overshooting is not the same for different physical quantities following our dynamic theory of convection, and this leads to some troubles in understanding and estimation of overshooting. Followed by the great success of helioseismology, people are expecting to draw a firm conclusion to the long debated overshooting distance at the bottom of the solar convective zone using the helioseismology method. Gough & Sekii (1993) reported that they cannot find any definite evidence for the existence of overshooting in the Sun; while others gave an upper limit of  $0.05\text{--}0.25H_P$  (Roxburgh & Vorontsov 1994, Monteiro et al. 1994, Christensen-Dalsgaard et al. 1995, Basu & Antia 1991, Basu 1997). Such results are understandable. Indeed, what the technique of helioseismology tests is the (adiabatic) sound speed in the Sun, while the sound speed is determined by the  $P$ - $T$  structures. In the overshooting zone, however, convective flux is negligible. That is why the overshooting below the bottom of the solar convective zone has not been detected by helioseismic diagnosis. From fig. 2, it is clear that the relative difference in sound speed between the local and non-local solar models is less than 1%. Such tiny differences were indeed detected by the inversion of adiabatic sound speed in helioseismology (Basu 1997), however the observed abrupt increase of the adiabatic sound speed at the bottom of solar convective zone was not correctly attributed to the non-local overshooting. In fact, convective flux changes its sign when crossing the boundary of convective zone, becoming negative in the overshooting zone ( $L_c < 0$ ); in there the radiative flux  $L_r$  will be even larger than the total flux of the Sun ( $L_\odot$ ). In the overshooting zone, the temperature gradient will overtake the radiative counterpart  $\nabla > \nabla_{rad}$  (see fig. 4). As a result, the temperature at the bottom of solar convective zone will rise up, just as what has been detected by helioseismology technique.

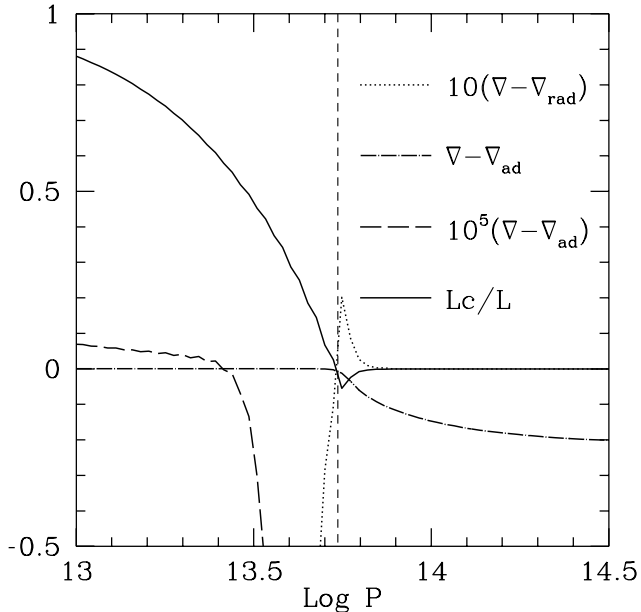


**Figure 4.** The super-adiabatic temperature gradient  $\nabla - \nabla_{ad}$ , super-radiative temperature gradient  $\nabla - \nabla_{rad}$  and the fractional convective flux  $L_c/L$  versus  $\log P$  in the lower convective and overshooting zones for a non-local convection model of the Sun.

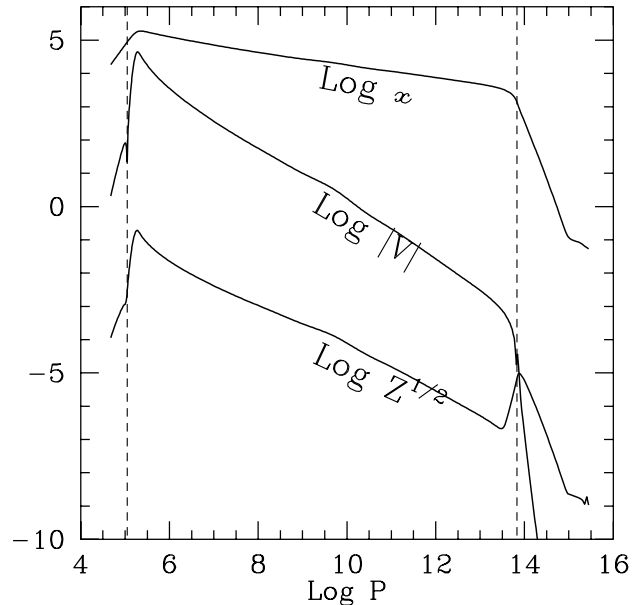


**Figure 6.** The auto- and cross-correlations of turbulent velocity and temperature  $x$ ,  $Z^{1/2}$  and  $V$  versus depth ( $\log P$ ) for a non-local convection model of the Sun. The vertical dashed lines indicate the upper and lower boundaries of the convective zone.

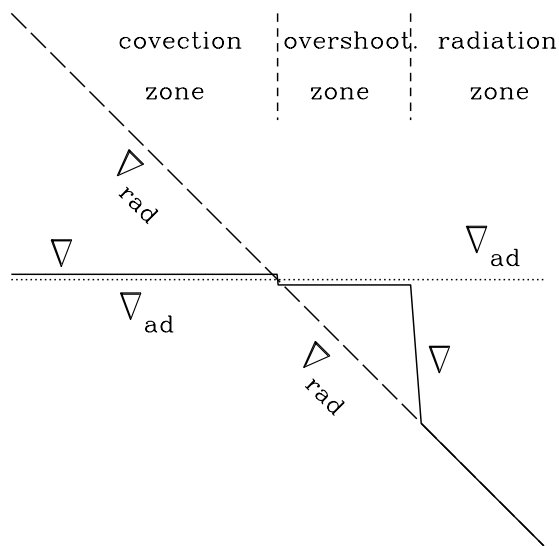


**Figure 5.** A sketch of the lower convective and overshooting zones in the usual phenomenological non-local mixing length theory (Monteiro et al. 2000).

Gough & Sekii (1993) measured the extension of overshooting at the bottom of solar convective zone following a picture of the overshooting zone made by the phenomenological non-local mixing length theory, which is illustrated in fig. 5. In the unstable zone, the temperature gradient is slightly higher than the adiabatic one, while being slightly lower in the overshooting zone. After a distance of an over-

shooting length  $d_{ov}$ , the temperature gradient switches suddenly to the radiative from adiabatic, making a discontinuity in temperature gradient at the bottom of the overshooting zone. The jump size of the temperature gradient is proportional to the overshooting distance  $d_{ov}$ . Such a discontinuity in temperature gradient is exactly what Gough & Sekii used to detect the overshooting distance  $d_{ov}$ . It is the implicit assumption of full (either positive or negative) correlation between turbulent velocity and temperature fluctuations that makes the misunderstandings of overshooting zone in the non-local mixing length theory (Xiong 1985, Petrovay & Marik 1995). In reality, however, the turbulent velocity-temperature correlation decreases very quickly and approaches zero near the lower boundary of the solar convective zone where convective energy transfer is very efficient, as demonstrated in fig. 1. Therefore, there is no similarity in the structure overshooting zone between the phenomenological non-local mixing length theory and the dynamic theory of non-local convection. In our view, the temperature gradient has already been smaller than the adiabatic one ( $\nabla < \nabla_{ad} < \nabla_{rad}$ ) before reaching the lower boundary of convective zone. The convective flux becomes negative passing through the boundary, therefore the temperature gradient  $\nabla$  is smaller than the adiabatic temperature gradient  $\nabla_{ad}$  and higher than the radiative one  $\nabla_{rad}$  ( $\nabla_{ad} < \nabla < \nabla_{rad}$ ). The temperature gradient changes continuously instead of abruptly from  $\nabla_{ad}$  to  $\nabla_{rad}$ . The structure of the overshooting zone in our dynamic theory of non-local convection is shown in fig. 4. In the overshooting zone under the convective zone, there is a narrow ( $\sim 0.25H_P$ ) and weakly super-radiative region. Actually, the overshooting zone is nearly radiative rather than nearly adiabatic. Therefore, it is not a surprise why Gough & Sekii (1993) could not find any firm evidence for the existence of the

**Table 1.** The e-folding lengths.

M/M <sub>⊙</sub>	upper oversh. zone			lower oversh. zone			Li	Dcut
	x	z	V	x	z	V		
0.800	0.47	0.36	0.20	0.25	0.25	0.080	0.26	0.30
0.850	0.48	0.36	0.21	0.25	0.25	0.081	0.36	0.38
0.900	0.50	0.35	0.20	0.25	0.25	0.082	0.42	0.54
0.925	0.50	0.36	0.21	0.25	0.25	0.069	0.50	0.58
0.950	0.50	0.33	0.20	0.26	0.25	0.076	0.60	0.69
0.975	0.49	0.33	0.20	0.31	0.31	0.104	0.67	0.74
1.000	0.50	0.32	0.20	0.29	0.31	0.093	0.85	0.91
1.025	0.63	0.30	0.21	0.29	0.29	0.096	1.05	1.11
1.050	0.52	0.30	0.19	0.30	0.36	0.092	1.25	1.33
1.075	0.60	0.30	0.21	0.38	0.38	0.114	1.64	1.69

overshooting under the bottom of solar convective zone. We can further justify that the methods based on stellar thermal ( $P$ - $T$ ) structure will all under-estimate the true overshooting distance. In the lower overshooting, the turbulent velocity-temperature correlation is very small, and convective energy transfer in there is negligible. The overshooting distance detected by convective energy flux will be far smaller than that is represented by the turbulent velocity and temperature fields. It follows from fig. 6 that, in the overshooting zones either at the surface or bottom of the solar convective zone, the overshooting distances of turbulent velocity and temperature are both very extended, their e-folding lengths of overshooting are given in table 1. Our theoretical e-folding length agrees fairly well with those derived from observations of the solar granular field (Keil & Danfield 1978, Nesic & mattig 1989, Komm, Mattig & Nesic 1991).

The overshooting distance in terms of stellar evolution is the extension of the non-local convective mixing of chemical elements. Obviously, it is neither that of convective energy transfer nor those of turbulent velocity and temperature fluctuations. Calculations of massive star evolution under our complete non-local theory of convection shown that the non-local convective mixing overshoots a very extended distance (Xiong 1986).

Although the overshooting at the bottom of the solar convective zone cannot be observed directly, we fortunately have another excellent indicator, which is the Lithium abundance of the Sun and solar type stars, for the extension of overshooting. No matter how disputed the mechanism of Lithium depletions in the atmospheres of solar type stars is, it can provide, at least, an upper limit for the extension of overshooting zone in these stars. As it is well known,  ${}^7\text{Li}$  gets burnt due to reaction  ${}^7\text{Li}(P, \alpha){}^4\text{He}$  at a temperature of  $2.5 \times 10^6 \text{K}$ . The depth of the solar convective zone, as given by helioseismology, is  $r_c/R_\odot \approx 0.713$ , and the temperature at the bottom of the zone is  $T_c \approx 2.26 \times 10^6 \text{K}$  (Basu & Antia 1997, Christensen-Dalsgaard et al. 1991). This temperature is not high enough to burn Lithium, without overshooting (bringing Lithium deeper to higher temperatures) there will be no depletion of Lithium in the Sun. It is the overshooting that brings Lithium to the burning region at a higher temperature, and causes depletion. Figs. 7a-7d show the Lithium abundance depletions due to overshooting for  $M=0.90, 0.95, 1.00$  and  $1.05M_\odot$  stellar models as functions of depth ( $\log P$ ), when the effect of evolution is not considered. The dashed lines in the plots indicate the boundary of convective zone. As from fig. 7c, there is a gradually accel-

erating reduction of Lithium abundance in the overshooting zone. In the upper part of the overshooting zone, the mixing caused by non-local convection is very efficient, the abundance keeps the same as in the convectively unstable zone for about  $0.4 H_P$  in length downwards. It is then followed by a partially mixed region where Lithium abundance is reduced quicker toward the center and vanishes suddenly, such a partial mixing region is about  $0.5H_P$  in depth. Even deeper is the non-mixing zone. If the overshooting distance is taken as the e-folding length of the abundance from the bottom of the convective zone, it reads about  $0.83H_P$ ; otherwise if we count the deepest bottom of the mixing process, it reads about  $0.9H_P$  for the solar model.

The equation for the conservation of Lithium abundance can be written as,

$$\frac{1}{C} \frac{\partial C}{\partial t} = -\frac{1}{C} \frac{\partial}{\partial M_r} (4\pi r^2 \rho U) - q, \quad (35)$$

where  $C$  is the Lithium abundance by mass,  $q$  is burning rate of Lithium, and  $U$  is the correlation of the radial component of turbulent velocity  $w'_r$  and the turbulent fluctuations of Lithium abundance defined as,

$$U = \overline{w'_r C}, \quad (36)$$

therefore  $4\pi r^2 \rho U$  is the total flux of convective mixing of Lithium passing through the sphere of radius  $r$ , and the first term on the right hand side of eq. (35) is the rate of variation of Lithium abundance due to non-local convective mixing. It follows from fig. 6 that, in the overshooting zone, turbulent velocity decreases nearly exponentially. The non-mixed region does not mean there is no mixing at all. In our picture, mixing is always there, the only difference is quantity of mixing. When the non-local mixing timescale  $\tau_{mix}$  becomes much longer than the nuclear timescale  $\tau_{nuc}$  of depletion, i.e. the non-local mixing cannot feed fresh Lithium into the burning zone, Lithium abundance vanished abruptly. Figs 8a-d give these two terms on the right hand side of eq. (35) and their sum (the depletion rate of Lithium) versus depth near the lower boundary of convective zones for 0.90, 0.95, 1.00 and  $1.05M_\odot$  main sequence stellar models respectively. The unit for these quantities are all  $yr^{-1}$ . The vertical dashed line locates the lower boundaries in these models. As clearly shown in fig. 8, the depletion of Lithium starts at  $T \sim 2.5 \times 10^6 \text{K}$ , and it goes up very quickly as temperature increases (being proportional to the 21st power of temperature). In the whole envelopes of these models,  $U < 0$ , this means that convection keeps feeding Lithium from outer into inner layers in order to supply the depletion at the burning zone. In the convectively unstable zone (where  $q$  is extremely small), convective mixing is very efficient,  $d(4\pi r^2 \rho U)/dM_r$  is nearly constant (see fig. 8). Towards the deep interior, the nuclear burning rate  $q$  goes up abruptly. In the upper part of the overshooting zone, mixing due to convective overshooting is still efficient enough to compensate the depletion due to nuclear burning, therefore the Lithium abundance profile is still horizontal (see figs. 7 and 8). At the lower part of the overshooting zone, however, the convective overshooting mixing (the dotted lines in fig. 8) can no longer support the balance between mixing and depletion (long dashed lines in fig. 8).  $-\frac{1}{C} d(4\pi r^2 \rho U)/dM_r - q$  decrease abruptly towards the center, corresponding to Lithium abundance dropping off in fig. 7. This means the boundary of overshooting zone is



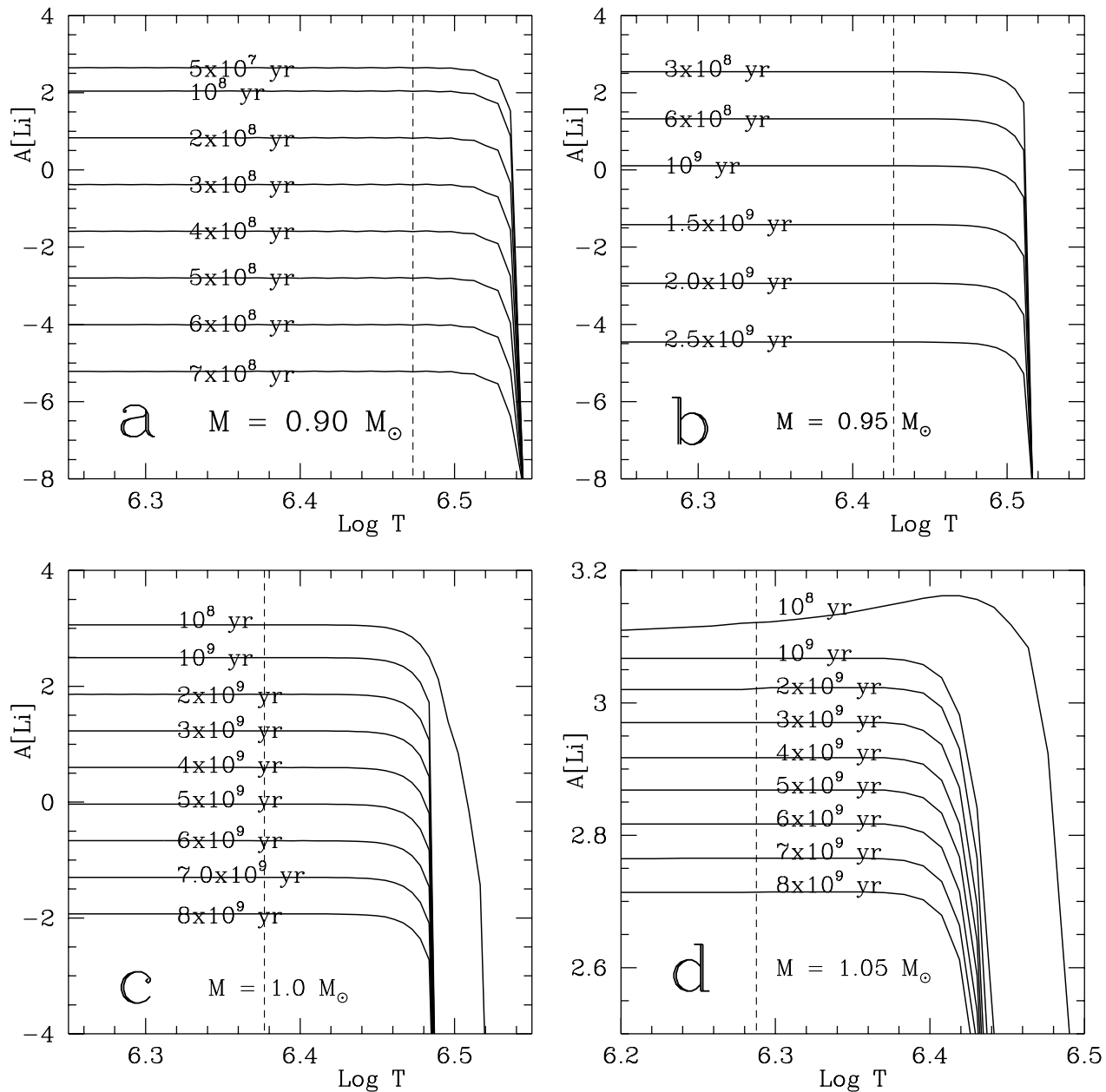


**Figure 7.** The Lithium abundance versus depth ( $\log T$ ) and age (labeled on the curves) for main sequence stars. The dashed vertical line indicates the location of the lower convective boundary. Evolution is not considered in the calculations. a).  $M=0.90M_{\odot}$ ; b).  $M=0.95M_{\odot}$ , c).  $M=1.0M_{\odot}$  and d).  $M=1.05M_{\odot}$ .

reached at this place. For the  $M=0.90M_{\odot}$  star, convective zone is very deep with its bottom already at the burning region of Lithium, this may leads to a shallower overshooting zone. Toward higher masses, convection becomes shallower, and the bottom of the zone goes farther away from the region of burning (see figs. 8c–d), the overshooting zone is then becoming more extended. Fig. 9 presents the overshooting distance  $d_{ov}$  measured by Lithium depletion as a function of stellar mass, from which it is clear that the overshooting distance  $d_{ov}$  increases as stellar mass increases, going from  $0.26H_P$  for  $M=0.80M_{\odot}$  to  $1.65H_P$  for  $M=1.075M_{\odot}$ . The overshooting distance defined by dropping off of Lithium abundance by a factor of  $e$  is shown in the 8th column of ta-

ble 1, while that defined by the distance from the boundary of convective zone to where Lithium becomes zero is given in the last column of table 1. It is clearly from figs. 7a–d that Lithium abundance vanishes very quickly after the  $e$ -folding depletion, the distance between them is less than  $0.1H_P$ . Completely different from the Lithium abundance profile in fig. 7, turbulent velocity ( $x$ ), temperature fluctuation ( $Z^{1/2}$ ) and velocity–temperature correlation ( $V$ ) decrease exponentially with depth in the overshooting zone. The  $e$ -folding distances determined from the curves are given in the 2nd–4th columns (for the upper part of overshooting zone), and 4th–7th columns (the lower part of overshooting zone). The  $e$ -folding distances given by turbulent velocity and temper-

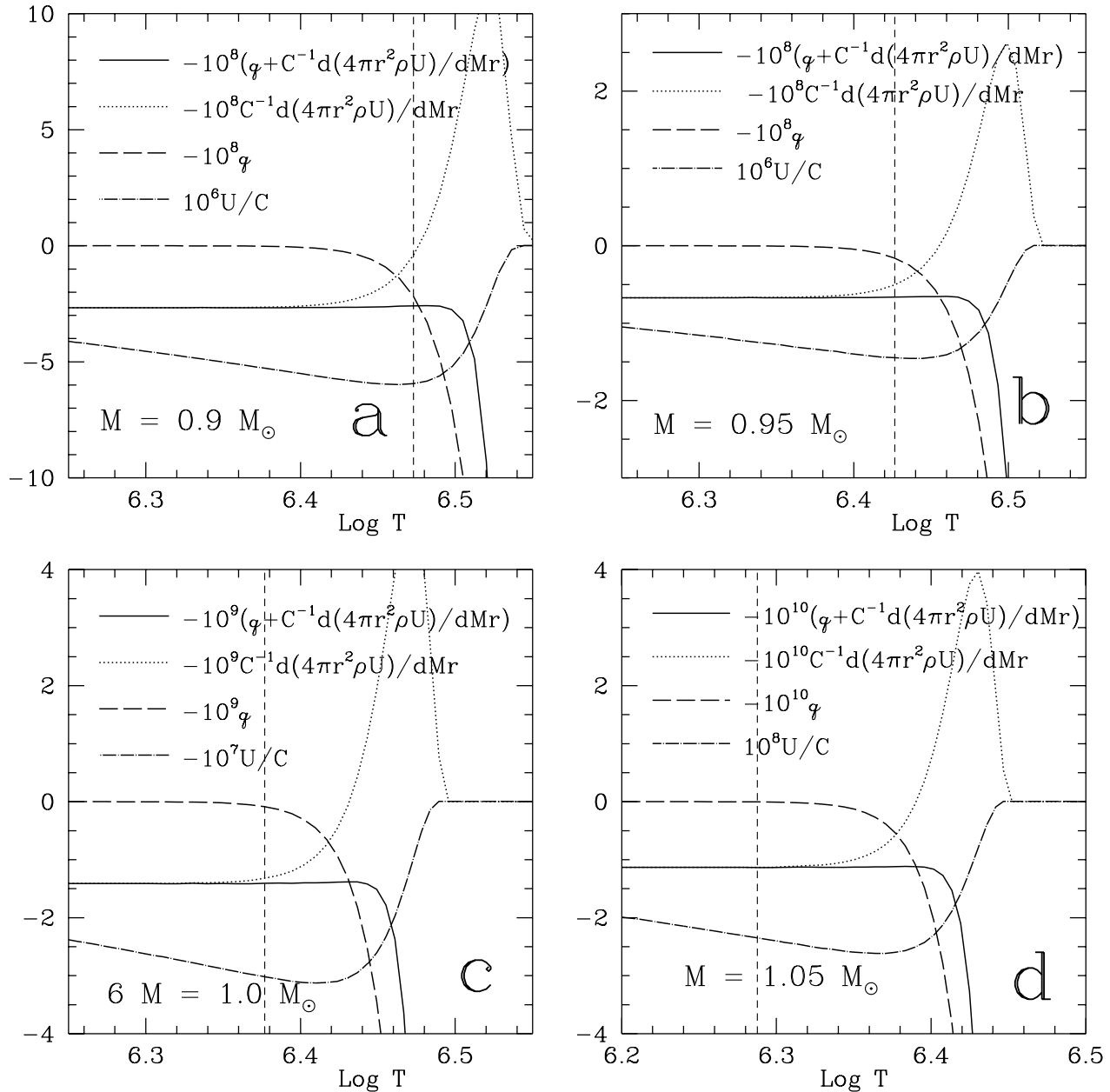


**Figure 8.**  $U/C$  ( $\text{sec}^{-1}$ ), burning rate of Lithium  ${}^7\text{Li}$  ( $\text{yr}^{-1}$ )  $q$ , change rate of convective diffusion for Lithium  $\eta = -\frac{1}{C} \frac{\partial}{\partial Mr} (4\pi r^2 \rho U)$  ( $\text{yr}^{-1}$ ) and  $\eta - q$  versus depth. The dashed line indicates the lower boundary of the convective zone. a).  $M=0.90M_{\odot}$ ; b).  $M=0.95M_{\odot}$ , c).  $M=1.0M_{\odot}$  and d).  $M=1.05M_{\odot}$ .

ature fields are very close to the analytic asymptote in our theory (Xiong 1989b). They hardly change with stellar mass, and are rather different from the e-folding distances defined by Lithium depletion. The upper and lower overshooting zones are a bit different in terms of these e-folding distances, this is due to the fact that, in the overshooting zone above the convective zone, gas density is low so that the effective Peclet number  $P_e \ll 1$ , and convective energy transfer is inefficient; while on the contrary, in the overshooting zone attach to the bottom of the convective zone,  $P_e \gg 1$ , and convection is highly efficient. These arguments mark the distinct properties of the velocity–temperature correlation in the upper and lower overshooting zones: in the surface over-

shooting zone,  $R_{VT} \sim -1$ , while in the bottom overshooting zone,  $R_{VT} \sim -0.0$ . When plotting fig. 1,  $R_{VT}$  has been magnified in order to show the details. In fact, we should have  $-10^3 < R_{VT} < 0$  in the lower overshooting zone, so that it is completely buried in the solid line of  $(L_c/L)$ .

#### 4 SUMMARY AND DISCUSSIONS

Detailed discussions on the definition of the boundary of convective zone, and the distance of convective overshooting are presented in this paper. The main results can be summarized in the following:

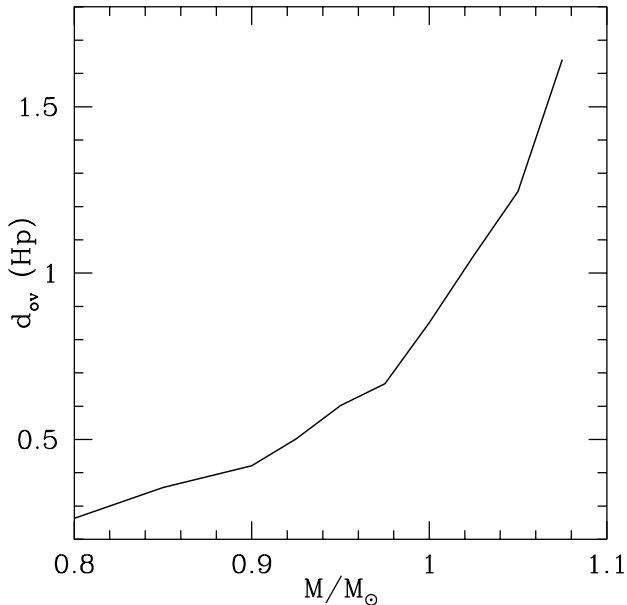


**Figure 9.** The overshooting distance as a function of stellar mass, as derived from Lithium depletion in solar type stars.

(i) Choosing the place where the convective flux (or equivalently the turbulent velocity–temperature correlation) changes its sign as the boundary is the most proper and convenient. Where the convective flux is greater than zero is the convectively unstable zone, while it is the overshooting zone when the convective flux is smaller than zero. The convective zone defined as such not only makes the local and non-local convection models with the same depth of convection zone to have similar structures, but also to have very clear physical meanings: convective zone is the buoyant force driving zone for convective motion, while the overshooting zone is the dissipation zone against convective motion, which can only be supported by non-local convective diffusion;

(ii) It is not quite right to talk about a general overshooting distance for stellar convection. The distance of overshooting is different for different physical quantities. The effect of overshooting for convective energy transfer, for instance, is not important. However, the overshooting distances of turbulent velocity and temperature fluctuations are quite extended, the e-folding lengths can reach 0.25–0.5 $H_p$ . The overshooting distance in terms of stellar evolution is the extent of convective mixing of chemical elements. From the example set by the depletion of Lithium in solar type stars, it is found that convective mixing of matter happens in stellar evolutionary (nuclear) timescales, and is very efficient. Very extended and weak overshooting can still induce fairly efficient mixing in a very long timescale of evolution. Therefore we anticipate a very extended overshooting for mixing of matters, the e-folding lengths of which is generally larger than that of turbulent velocity and temperature. The one in massive stellar model, for instance, can reach 1 pressure scale height (Xiong 1986).

(iii) The problem of Lithium depletion in solar type stars is a special case of overshooting mixing that moves Lithium to the burning region from surface. Under such circumstance, overshooting distance depends on the location of

convective zone relative to that of Lithium burning region. Obviously, such conclusion cannot be simply generalized to the case of the core nuclear reaction. For Lithium depletion in solar type stars, the convective zone becomes shallower for higher masses, and Lithium depletion becomes slower (longer timescale), and this makes the extended overshooting tail to be efficient in mixing, and the mixing range to become more extended. As a result, the overshooting distance detected by Lithium depletion in solar type stars becomes larger for increasing stellar mass. In fact, this indicates that mixing of matter becomes more extended for increasing nuclear burning timescales.

### ACKNOWLEDGEMENTS

The Chinese National Natural Science Foundation (CNNSF) is acknowledged for support through grants 10573022, 10173013, 10273021 and 10333060.

### REFERENCES

- Basu, S. & Antia, H.M., 1994, MNRAS, 269, 1137  
 Basu, S. & Antia, H.M., 1997, MNRAS, 287, 189  
 Basu, S., 1997, in Proc. IAU Symp. 181, Sounding solar and stellar interiors, eds. J. Provost, F-X Schmider (Kluwer, Dordrecht), p. 137  
 Böhm-Vitense, E., 1958, Astrophysik, 46, 108  
 Bressan, A., Bertelli, G. & Chiosi, C., 1981, A&A, 102, 25  
 Canuto, V.M., 1993, ApJ, 416, 331  
 Canuto, V.M. & Dubovikov, M., 1998, ApJ, 493, 834  
 Chiosi, C. & Summa, C., 1970, ApSS, 8, 478  
 Christensen-Dalsgaard, J., Monteiro, M.J.P.F.G., Thompson, M.J., 1995, MNRAS, 276, 283  
 Christensen-Dalsgaard, J., Gough, D.O. & Thompson, M.J., 1991, ApJ, 378, 413  
 Gough, D.O. & Sekii, T. 1992, in ASP Conf. Ser. Vol 42, ed. T.M. Brown, p.117  
 Grossman, S.A., Narayan, R. & Arnett, D., 1993, ApJ, 407, 284  
 Grossman, S.A., 1996, MNRAS, 279, 305  
 Keil, S.L. & Canfield, R.C., 1978, A&A, 70, 169  
 Komm, R., Mattig, R.W. & Neiss, A., 1991, A&A, 243, 251  
 Kuhfuss, R., 1986, A&A, 160, 116  
 Kupka, F., 2003, in Modelling of Stellar Atmosphere, IAU Symp. 210, eds N. Piskunov, W.W. Weiss & D.G. Gray, p.143 (Pub. ASP)  
 Leighton, R.B., Neyes, R.W. & Simon, G.W., 1962, ApJ, 135, 474  
 Monteiro, M.J.P.F.G., Christensen-Dalsgaard, J. & Thompson, M.J., 1994, A&A, 283, 247  
 Monteiro, M.J.P.F.G., Christensen-Dalsgaard, J. & Thompson, M.J., 2000, MNRAS, 316, 165  
 Nesis, A. & Mattig, W., 1989, A&A, 221, 130  
 Roxburgh, I.W. & Vorontsov, S.V., 1994, MNRAS, 268, 880  
 Salucci, G., Bertello, L., Gavallini, F. Ceppatelli, G. et al., 2004, MNRAS, 285, 322  
 Schwarzschild, M. & Harm, R., 1958, ApJ, 128, 348  
 Spiegel, E.A., 1963, 216  
 Stothers, R., 1970, MNRAS, 151, 65  
 Travis, L.D. & Matsushima, S., 1973, ApJ, 186, 975  
 Ulrich, R.K., 1970, ApSS, 7, 183  
 Unno, W., Kondo, M. & Xiong, D.R. 1985, PASJ, 37, 235  
 Xiong, D.R., 1977, AcASn, 18, 86  
 Xiong, D.R., 1978, ChA, 2, 118  
 Xiong, D.R., 1981a, SciSn, 23, 1139  
 Xiong, D.R., 1981b, AcASn, 22, 356

- Xiong, D.R., 1982, ChA, 6, 43  
Xiong, D.R., 1985, A&A, 150, 133  
Xiong, D.R., 1986, A&A, 167, 239  
Xiong, D.R., 1989a, A&A, 209, 126  
Xiong, D.R., 1989b, A&A, 213, 176  
Xiong, D.R. & Cheng, Q.L., 1992, A&A, 254, 362  
Xiong, D.R., Deng, L. & Cheng, Q.L., 1998, ApJ, 499, 355  
Xiong, D.R., Cheng, Q.L. & Deng, L., 1998, ApJ, 500, 449  
Xiong, D.R. & Deng, L., 2001, MNRAS, 324, 243  
Xiong, D.R. & Deng, L., 2007, MNRAS, in press